Experimental Investigations on Geometrical Resolution of Optical Transition Radiation (OTR)

X. Artru, M. Castellano, L. Catani, R. Chehab, D. Giove, K. Honkavaara, P. Patteri, M. Taurigna–Quere, A. Variola, L. Wartski

Experimental investigations on geometrical resolution of optical transition radiation (OTR)

X.Artru[1], M.Castellano[2], L.Catani[2], R.Chehab[3*], D.Giove[4], K.Honkavaara[3,5], P.Patteri[2], M.Taurigna-Quere[3], A.Variola[3], L.Wartski[6]

[1] Institut de Physique Nucléaire de Lyon IN2P3-CNRS, 69622 Villeurbanne Cedex, France
[2] Istituto Nazionale di Fisica Nucleare, Laboratori Nazionali di Frascati, 00044 Frascati, Italy
[3] Laboratoire de l'Accélérateur Linéaire IN2P3-CNRS, Université de Paris-Sud, 91405 Orsay Cedex, France
[4] Istituto Nazionale di Fisica Nucleare, LASA, 20090 Segrate (Milano), Italy
[5] Helsinki Institute of Physics, P.O.Box 9, 00014 University of Helsinki, Finland
[6] Institut d'Electronique Fondamentale, Bat.220, 91405 Orsay Cedex, France

Abstract

Optical Transition Radiation (OTR) provides an attractive method for diagnostics on electron/positron beams of small dimensions at high energies (GeV). However, some limits on the geometrical resolution at very high energies have been often discussed in the literature and a minimum value given by '$\gamma\lambda$' has been invoked. In order to bring an experimental contribution to the problem, systematic measurements of electron beam profiles, in the energy range of 1-2 GeV and at optical wavelength between 400 and 700 nm, have been carried out at the Orsay 2 GeV Linear Accelerator. OTR emitted from an Aluminium foil at a 30° incidence angle was collected by a two-lens telescope and recorded by an intensified CCD camera. The OTR

beam profiles were compared to the profiles obtained by a SEM Grid having a resolution better than 0.5 mm.

After a theoretical introduction presenting the different resolution limits, which can be invoked with diffraction phenomenon, and a presentation of our calibration procedure, the experimental results are presented and compared to these limits. They show that the resolution in OTR measurements is definitely better than the already invoked $\gamma\lambda$ -limit. For a small size electron beam an rms beam width as small as 170 μm, compared to $\gamma\lambda = 2.5$ mm (E= 2 GeV and $\lambda = 650$ nm), has been measured. Our theoretical analysis also provides a more precise evaluation of the resolution power of OTR, which depends on the sensitivity of the detector; this could be of interest for much higher energies.

1 Introduction

In order to ensure high luminosities in e^+e^- Linear Colliders (LC) or good brilliances in Free Electron Lasers (FEL), strong constraints are put on the beam characteristics. Therefore, high intensity beams with small emittances both in the longitudinal direction and the transverse plane are required at such facilities. These requirements necessitate accurate beam diagnostics in several places upstream of the interaction point or the undulator magnet. In the present projects the transverse dimension of the beam, at these locations, can reach the size of some tens of microns and the duration of the bunch can be as short as some picoseconds or even less [1]. This is a typical situation for the TESLA collider [2] as for the SASE (Self Amplified Spontaneous Emission) FEL [3] that will be realized at the Tesla Test Facility [4]. Among the various systems already used on electron linacs, the transition radiation monitors associated to CCD, Streak Cameras or interferometers (for subpicosecond bunches) appear to have a good performance in measuring short bunches with small transverse dimensions. However, the ability to reach a resolution of some tens of microns at high energies (some GeVs or more) has to be checked, as far as the self-diffraction phenomenon can be invoked. This question has been a subject of debate; some authors [5,6] argued out difficulty to obtain a good resolution for submillimeter beam dimensions at multiGeV energies. Others estimated that such difficulties might not occur [7]. In the context of the future LC and FEL this problem is becoming an important issue. We have made a first experimental investigation of this problem and the results are presented here.

After a brief theoretical presentation of the problem, the experimental set-up and the calibration of the optical channel are described. The main results are then presented and discussed.

2 Theoretical background

The angular distribution of transition radiation on a perfectly reflecting metallic surface is of the form [8]

$$I(\theta) = \omega \frac{dN}{d\omega\, d\Omega} = \frac{\alpha}{\pi^2} \left(\frac{\theta}{\gamma^{-2} + \theta^2} \right)^2 , \qquad (1)$$

1

where $\gamma = E/m >> 1$ in natural units ($\hbar = c = 1$) and $\theta << 1$ is the angle of the photon with respect to the electron velocity $\mathbf{v}$ (case of forward transition radiation) or its specular direction (case of backward transition radiation). Its integral is

$$\omega\frac{dN}{d\omega} = \frac{\alpha}{\pi}\left\{\ln[1 + (\gamma\theta_{\text{max}})^2] - 1 + [1 + (\gamma\theta_{\text{max}})^2]^{-1}\right\} \simeq \frac{2\alpha}{\pi}\ln(\gamma\theta_{\text{max}})\,, \quad (2)$$

where θ_{max} is of the order of $\pi/2$ or determined by the optical system. The distribution (1) is peaked on the cone of half-aperture $\theta = 1/\gamma$. Diffraction — equivalently, the Heisenberg uncertainty principle in the transverse phase space of the photon [9] — sets a lower limit on the size of the emitting zone at the surface of the foil :

$$\Delta b_i \geq \lambdabar /(2\Delta\theta_i) \qquad (i = x, y)\,, \quad (3)$$

where $\lambdabar = 1/\omega = \lambda/(2\pi) \sim 0.1\mu$m is the reduced observed wavelength, b_i and θ_i are the components of the impact parameter $\mathbf{b}$ and of the photon direction $\hat{\mathbf{n}}$ along the transverse directions $\hat{\mathbf{x}}$ and $\hat{\mathbf{y}}$. $\Delta\theta_i$ and Δb_i are the corresponding rms values. Concerning the application of transition radiation to the measurement of beam profiles, it has been pointed out [5,6] that the narrowing of the peak at increasing γ leads to a widening of the "self-diffraction" spot which may spoil the spatial resolution. Indeed, if one takes for $\Delta\theta$ the peak angle $1/\gamma$, then

$$\Delta\mathbf{b} \sim \gamma\lambdabar /2\,, \quad (4)$$

which gives a resolution ~ 0.5 cm at $\gamma \sim 10^5$. The situation, however, may be not so catastrophic :
- Firstly, at high γ, most of the photons are not emitted in the peak but in the tail of the angular distribution (1), and the mean square value of the angle is given by

$$< \theta^2 > = (\Delta\theta_x)^2 + (\Delta\theta_y)^2 \simeq \frac{(\theta_{\text{max}})^2}{2\ln(\gamma\theta_{\text{max}})}\,, \quad (5)$$

which is usually much larger than γ^{-2}.
- Secondly, the angular distribution (1) is obtained only if the electron follows a rectilinear uniform motion over a distance at least equal to the *formation length*

$$l_f(\theta) = \frac{1}{\pi}\frac{\lambda}{\gamma^{-2} + \theta^2}\,. \quad (6)$$

At the peak angle, this length is $l_f(\gamma^{-1}) = \gamma^2 \lambda$, which is of the order of 1 km at $\gamma \sim 10^5$. If the electron trajectory is bent or if it traverses an opaque material at distance l less than $l_f(\gamma^{-1})$ before the foil (case of backward transition radiation) or after the foil (case of forward transition radiation), the peak at $\theta = \gamma^{-1}$ is absent and replaced by a wider structure (this is in particular the case in the Wartski interferometer [10]).

In the following we will assume, as in the experiment reported below, that there is a sufficient electron path length for the formation of the peak and attempt to estimate the resolution limit in this case. From a microscopic point of view, backward OTR is generated by the collective motion of the metallic electrons in response to the transient Coulomb field of the incident particle. These electrons emit coherently electromagnetic waves of amplitude

$$\tilde{\mathbf{A}}(\omega, \mathbf{k}) \propto e\, \mathbf{k}_\perp / (\omega^2 \gamma^{-2} + \mathbf{k}_\perp^2)\,, \tag{7}$$

where $\mathbf{k}_\perp = (\omega \theta_x, \omega \theta_y)$ is the transverse momemtum of a photon relative to the specular direction of the electron. The Fourier transform $\mathbf{A}(\omega, \mathbf{b})$ of $\tilde{\mathbf{A}}$ with respect to $\mathbf{k}_\perp$ gives the amplitude of the source as a function of the impact parameter $\mathbf{b}$ (transverse distance to the incident particle). Squaring $\mathbf{A}(\omega, \mathbf{b})$, one obtains the intensity profile of the elementary source, considered as located on the foil :

$$I(\mathbf{b}) = \omega \frac{dN}{d\omega\, d^2\mathbf{b}} \simeq \frac{\alpha}{\pi^2} \frac{\omega^2}{\gamma^2} K_1^2 \left(\frac{\omega b}{\gamma} \right) \Theta(b - b_{\min}) \tag{8a}$$

$$\simeq \frac{\alpha}{\pi^2} \frac{1}{\mathbf{b}^2} \Theta(b - b_{\min})\, \Theta(b_{\max} - b)\,, \tag{8b}$$

where K_1 is a Bessel function of second kind, $b_{\min} \sim \lambda / \theta_{\max}$ and $b_{\max} \sim \gamma \lambda$. Apart from the cut-off function $\Theta(b - b_{\min})$, one can recognize in Eq.(8a) the Weizsäcker - Williams distribution of quasi-real photons [11]. Eq.(1) is the corresponding distribution in the transverse momentum representation [12]. Indeed, transition radiation (in the backward case at least) can also be viewed as a reflection of the cloud of the quasi-real photons on the metallic foil. $\Theta(b - b_{\max})$ and $\Theta(b - b_{\min})$ are phenomenological cut-offs functions, with $b_{\min}$ and $b_{\max}$ reciprocal to the cut-offs in the photon transverse momentum, $\mathbf{k}_{\perp \max} = \omega\, \theta_{\max}$ and $\mathbf{k}_{\perp \min} = \omega\, \theta_{\min}$ where $\theta_{\min} \sim \gamma^{-1}$. Note the similar power law decrease in b and θ and that cut-offs are in the ratio

$$\frac{\theta_{\max}}{\theta_{\min}} = \frac{b_{\max}}{b_{\min}} = \gamma \theta_{\max}\,. \tag{9}$$

3

Without the cut-off b_{min} the photon density would diverge at $\mathbf{b} = 0$, whereas, for reason of symmetry, it has to vanish there. More systematic treatments of the diffraction effect due to diaphragms are given in Refs.[13,14].

$I(\mathbf{b})$ is the OTR spatial profile for one incident particle which has to be convoluted with the real beam profile to get the observed one, focusing the optical system on the foil. It contains only the self-diffraction effect if one takes $\theta_{max} \sim \pi/2$. If one takes θ_{max} to be the angular aperture of the optics, $I(\mathbf{b})$ takes also into account the Fraunhofer diffraction by the diaphragm [1].

In Ref.[14] the spatial resolution of OTR is assumed to be given by the FWHM value of the distribution $I(\mathbf{b})$, which is found to be about 3 times larger than the intrinsic resolution of the optical system, and it is concluded that the resolution does not depend on the beam energy. Instead of the FWHM, one could choose the mean square value of $\mathbf{b}$. It can be calculated directly from Eq.(7), using the correspondance principle $\mathbf{b} \leftrightarrow i \nabla_{\mathbf{k}_\perp}$. One gets [2]

$$< \mathbf{b}^2 > \, \simeq \, \lambdabar^{\,2} \, \frac{\int_{-\infty}^{\infty} d\theta_x \, d\theta_y \, \sum_{i,j} \, |\, \partial_i \, [\theta_j/(\gamma^{-2} + \theta^2)] \,|^2}{\int_0^{\theta_{max}} 2\pi \, \theta \, d\theta \, |\, \theta/(\gamma^{-2} + \theta^2) \,|^2} \, \simeq \, \frac{4}{3} \, \frac{(\gamma \lambdabar \,)^2}{2 \ln(\gamma \theta_{max})} . \tag{10}$$

This result depends on the beam energy but is better than Eq.(4). It can be roughly understood knowing that the $1/\gamma$ peak represents a fraction of the order of $1/(\ln(\gamma \theta_{max}))$ of the total flux. For a 2 GeV electron, $\lambda = 0.65 \, \mu$m and $\theta_{max} = 0.04$ radian, Eq.(10) predicts $\Delta b_x = \Delta b_y = (0.5 < \mathbf{b}^2 >)^{1/2} \simeq 104 \, \mu$m, whereas Eq.(24) of Ref.[14] gives a FWHM of 23.4 μm.

The big difference between the rms and the FWHM is due to the nongaussian form of $I(\mathbf{b})$. This distribution presents a long tail which leads to a large rms value, therefore pessimistic; conversely the FWHM is much smaller and should be optimistic. In fact the spatial resolution power of OTR cannot be characterized by just one parameter. A complete description is provided by the modulation transfer function $MTF(\nu)$ where ν is the spatial frequency. This function is the 2-dimensional Fourier transform of the intensity $I(\mathbf{b})$

---

[1] Eq.(8b) does not contain the oscillations (fringes) which occur in the case of a sharp-edged diapragm. It assumes an *apodized* diapragm.

[2] In this equation we integrate the numerator over the whole (θ_x, θ_y) plane and neglect the derivatives of the cut-off function $\Theta(\theta_{max} - \theta)$. This is not justified not for a sharp edge of the diaphragm but for a smooth (apodized) one, with a transition region broader than γ^{-1}.

for one particle, normalized to $MTF(0) = 1$. Introducing the modulation wavelength $\lambda_{\mathrm{mod}} = 2\pi \lambdabar_{\mathrm{mod}} = \nu^{-1}$ and taking the approximation of Eq. (8b) (with smooth cut-offs), we have

$$MTF \simeq 1 \quad \text{for } \lambdabar_{\mathrm{mod}} > b_{\max},$$

$$MTF \simeq \frac{\ln(\theta_{\max} \lambda_{\mathrm{mod}}/\lambda)}{\ln(\gamma \theta_{\max})} = \frac{\ln(\lambdabar_{\mathrm{mod}}/b_{\min})}{\ln(b_{\max}/b_{\min})} \quad \text{for } b_{\min} < \lambdabar_{\mathrm{mod}} < b_{\max}, \quad (11)$$

$$MTF \simeq 0 \quad \text{for } \lambdabar_{\mathrm{mod}} < b_{\min}.$$

For instance, beam details of the size $\lambdabar_{\mathrm{mod}} \sim b_{\min}^{2/3} b_{\max}^{1/3}$ are reproduced with a contrast of 1/3. Alternatively, $I(\mathbf{b})$ can be decomposed in a crude phenomenological way into a series of concentric disks of very different sizes, e.g.,

$$I(\mathbf{b}) \sim \frac{\alpha}{\pi^2} \sum_0^N b_n^{-2} \, \Theta(b_n - b), \quad (12)$$

with $b_n \sim b_{\min} \, e^{n/2}$ and $N \sim$ nearest integer $[2 \ln(b_{\max}/b_{\min})]$. Thus the resolution power of OTR depends not only on γ and on the angular acceptance of the optics but also on the sensitivity of the detector. We have considered backward OTR. Similar considerations apply to forward OTR.

Possible improvement of the OTR method. In order to conclude in an optimistic way, let us remark that, even when the peak is there (case $l > l_f(\gamma^{-1})$), it may be possible to prevent its bad influence on the spatial resolution by putting a mask which absorbs the photons emitted at θ less than some angle $\theta_{\mathrm{mask}} \gg \gamma^{-1}$ and let pass those emitted at $\theta \geq \theta_{\mathrm{mask}}$. This mask (preferrably apodized) should in principle be placed in the image focal plane of the optics (or one of the intermediate focal planes).

3 Experimental set-up

Our experimental set-up has been installed at the front end of the Orsay 2 GeV Linear Accelerator. The OTR radiator is a 20 microns thick aluminum foil mounted on a goniometer, which allows precise angular orientations as well as the complete removal of the foil. The electron beam impinges on the radiator with a 30° incidence angle and the light from backward transition

radiation is collected in the direction of the specular reflection. The set-up is shown in Fig.1.

The beam intensity is monitored by a toroid placed upstream of the radiator. A SEM Grid providing horizontal and vertical beam profiles with a resolution better than 0.5 mm is placed downstream of the goniometer.

The requirements for a small emittance beam (i.e. small beam dimensions and divergence) are fulfilled by means of two collimators placed upstream of the OTR radiator. Collimators are 60 meters apart and the closest one is situated at 40 meters from the radiator. At their locations, the beam aperture is restricted to 2 to 4 mm at full width. The possibility to close the collimators only in one direction enables us to use a flat beam. A quadrupole doublet, 30 meters upstream from the radiator, permits focusing of the beam. The beam energy can be varied from 1 GeV up to 2 GeV and the beam charge from $1 * 10^9$ to $2 * 10^{10}$ electrons/pulse for a 30 ns pulse width.

The OTR beam image is transmitted through a glass window (BK 7) to an optical channel composed of two lenses in a telescopic configuration with a magnification factor of 1/4. The first lens is an achromatic lens with a focal length of 1 m and a diameter of 8 cm and the second one a plano-convex lens with a focal length of 25 cm and a diameter of 14 cm. An intensified CCD camera is placed at the image plane of the foil. Optical interferential filters in the range of 400 - 700 nm (with a 40 nm or 80 nm FWHM bandwidth) are used in the measurements.

The alignment of the optics is provided by a He-Ne Laser and prior to each experimental session a control of the general alignment is performed by observing the image of the thermoionic gun cathode on the CCD camera.

4   Calibration of optical set-up

In order to quantify the performance of our optical set-up, we carried out some measurements on single components and on the reconstruction of the whole apparatus.

First it was necessary to calibrate the apparatus, i.e. to determine the ratio between the number of pixels on the image plane given by a frame grabber and the actual geometrical dimensions. The set-up (two lenses and the camera) was reconstructed on an optical rail and a point light source was created by means of a green LED and a diaphragm (with a diameter of

0.1 mm i.e. 0.025 mm in the image plane). The source has been assembled on a stepping motor driven stage, which garantees an accuracy of the order of 1 μm in movements over a range of 1.5 mm both in the horizontal and vertical directions. Many different image acquisitions, along with the stage position readings, have been performed at different places of the source in the image plane. We observed the peak distances both in the horizontal and the vertical direction and we obtained the following ratios: 0.097 mm/pixel in the horizontal direction and 0.064 mm/pixel in the vertical direction. Different ratios are due to the grabber acquisition.

After the calibration measurements, we measured the resolving power i.e. the capability to separate two closely spaced objects, using a simplified optical set-up. A detailed description of the followed procedures and a complete discussion on the experimental data is reported elsewhere [15].

Before these measurements we estimated the chromatic and spherical aberrations. Thanks to the lens quality and the narrow emission cone the effect on the beam image caused by the focal displacement due to the aberrations was in the order of 1 % causing a neglible effect on the resolution.

The camera behaviour was studied by using a classical methodology for optical apparatus. PSF, Point Spread Function (a 3 dimensional plot of point source image coordinates x, y and intensity I), and MTF, Modulation Transfer Function (the Fourier transform of PSF which gives the passband spectrum in spatial frequency of the optical system)[16], were the main elements of the analysis. A numerical value of the limiting resolution in a particular environment can be obtained by using a test target. A widely used design is the 3-bar target, attributable to the USAF in 1951 and described in ANSI (1969) [17]. Three bars of the same shape and space are spaced forming patterns of identical size. Each target element consists of two adjacent orthogonal patterns giving a particular object spatial frequency. There are four groups of six elements in each and the period variations between the groups is fixed in such a way that the period of the first element of each group is double of the previous. A measure of the Modulation Transfer Function (defined as a function of the ratio between the maximum and minimum intensity) for each single spatial frequency in a target as a function of the different frequencies gives the MTF of the imaging process.

The limit in the resolving power for a particular optical set-up can be defined as the spatial frequency that match to a predefined and accepted value of MTF and it is given in line pairs per millimeter. We obtained a

resolving power, at the limit of the MTF range (MTF $= 8*10^{-2}$), of the order of 12 pairs for millimeter (Fig.2). This means that the ultimate resolution of our system is of the order of 80 μm.

MTF values are strongly influenced by many conditions, like object illumination, and they depend on the behaviour of the optical set-up as a function of its characteristics. In our case we did not have a possibility to optimize object illumination, but we had to take into account the effect of the camera gain (i.e. the variable total intensity on the camera) in the determination of the camera resolution.

Variations in PSF versus the intensity were obtained in two different ways. We created a small light source by means of a red laser and a diaphragm. First we changed the applied voltage of the photocathode of the camera intensifier (i.e. the camera gain) and registered the FWHM size of the spot and then this measurement was confirmed by another experiment, in which we fixed the gain level and changed the laser intensity. The results of these two experiments were in agreement with each other. Fig.3 shows the spot size as a function of the camera gain.

We can conclude from the performed resolution tests that the intrinsic resolution of the camera is not the limiting factor for our measurements and that the resolution itself is a function of the total intensity, which is the relevant parameter rather than the camera gain.

5 Experimental results

We have performed several series of beam profile measurements varying three parameters: the electron beam energy, the voltage level of the photocathode of the CCD camera intensifier (the camera gain) and the observed optical wavelength (by means of filters). An image acquisition and analysis program enables us to obtain transverse profiles of the images and to derive the FWHM and rms widths.

The transverse beam profiles were summarized by their vertical and horizontal projections, measured on the image of the OTR spot. In all the cases the profiles showed rather good gaussian distributions, as can be seen in Fig.4 and Fig.5, which present vertical and horizontal profiles for low and high camera gain conditions at 2 GeV.

The measured beam widths were in good agreement with the results ob-

tained by the SEM Grid placed downstream of the OTR radiator. Fig.6 shows an example of the profiles on the SEM Grid.

Beam profile measurements have been performed at two different beam energies: 1.1 GeV and 2 GeV. In both cases and in the same experimental conditions we observed gaussian beam profiles and we did not notice any enlargement of the beam size with the energy; even we observed smaller sizes at 2 GeV than at 1.1 GeV, which could be attributed to the decrease of the beam emittance. [18]

Systematic measurement were performed at fixed spectral domain to test the dependence of the measured beam widths on the gain level of the intensified CCD camera. In the different runs we worked at different gain ranges depending on the beam intensity, background conditions and the chosen measurement scheme (i.e. measurement of the whole optical spectrum, use of an attenuator or a selection of a certain wavelength by means of a filter). In all the cases we determined the minimum gain needed to obtain a beam image and the maximum gain accepted by the internal protection system of the camera. We observed a clear correlation between the measured beam width and the chosen gain: for all the wavelengths both the horizontal and the vertical beam widths increased with the camera gain.

At a fixed gain value, beam widths were measured for different wavelengths (λ = 400 nm, 500 nm and 600 nm, $\Delta\lambda$ = 40 nm). We observed a weak dependence on the wavelength: the maximum width was measured for the wavelength of 500 nm; the widths for 400 nm and 600 nm were smaller. This behaviour coincides with the spectral response of the intensified CCD camera. [18]

In order to study the minimum beam spot size measurable by OTR, we concentrated our analysis on two series of data that were taken by varying the camera gain at two wavelength values of 450 nm and 650 nm ($\Delta\lambda$ = 80 nm). We worked at the maximum beam energy obtainable by the accelerator and the collimators and quadrupole focusing were optimized to give the minimum spot size. The two wavelengths were chosen at the two extremes of the spectral sensitivity of the camera.

According to the camera calibration measurements [15], a variation of the beam spot size as a function of the total intensity had to be expected. The variation of the intensity may originate from different sources; the main one is the camera gain, but also the spectral sensitivity of the camera, which is not equal for the two selected wavelengths, contributes, as well as the

fluctuations of the beam intensity from pulse to pulse.

As it is clear from the example of image shown in Fig.7, the beam is not round and it is also sligthly rotated. Thus, to evaluate the smaller spot size, we determined an ellipse of minimum area containing a given fraction of the total intensity and calculated the rms value of the distribution along the ellipse axes. The rms values are very sensitive to the distribution tails, which are rather strong in the high intensity images. Therefore, we decided to eliminate the tails by selecting the ellipse containing 95 % of the total intensity. On the other hand, this cut does not change the results for the lower intensity images. The obtained rms values of the distribution along the ellipse minor axis are plotted in Fig.8 as a function of the total intensity.

We have fitted the experimental data with a formula of the type

$$\sigma_{rms} = \sqrt{\rho^2 + aI^b}, \tag{13}$$

where ρ is the real beam dimension, I is the intensity and a and b are free parameters. The result is shown as a continuous line in Fig.8 and numerically in Table 1.

The resulting ρ value is substantially equal for the two wavelengths (450 and 650 nm) with an average value of 170 μm. This value can be compared to :

- the $\gamma\lambda$ limit in Ref.[5], which gives 2.5 mm at 2 GeV ($\lambda = 650$ nm).

- the $\gamma\lambda$ /2 limit given by Eq.(4), which is associated to the uncertainty principle, when we consider an angular resolution of $1/\gamma$; this limit is 202 μm for $\lambda = 650$ nm and $E = 2$ GeV.

- the value derived from Eq.(10) giving an rms resolution of 104 μm.

6 Conclusions

The experimental results obtained in the energy range of 1 to 2 GeV on the electron linear accelerator of Orsay showed, as foreseen from the theoretical approach, that the resolution is not limited by the $\gamma\lambda$ value. As already pointed out by D.W.Rule and R.B.Fiorito [7], the restriction of the angular aperture of the OTR to $1/\gamma$ is incorrect. That was also confirmed by our measurements.

The resolution, in the energy range explored, is not affected by the relative high γ values and does not show measurable variations from 1 to 2 GeV, as

already reported in Ref.[18]. The attainable resolution in OTR observations can, therefore, be much better than previously predicted. Our theoretical approach showed that the resolution of OTR depends not only on γ and on the angular aperture of the optics, but also on the sensitivity of the detector. The latter dependence has also been confirmed by our experimental observations.

OTR measurements at higher energies, by one order of magnitude, with submillimeter beam sizes should bring interesting information about the OTR resolution limits which should be met in the future linear colliders.

Acknowledgements

References

[1] Conceptual Design Report for Linear Colliders, G.Loew (editor) (1996).

[2] R.Brinkmann, "Status of the Design for the TESLA Linear Collider", Proceedings of 1995 Particle Accelerator Conference, May 1995, Dallas, p.674.

[3] R.Bonifacio, C.Pellegrini, I.M.Narducci, Opt.Commun. 50 (1984) 373.

[4] Tesla Test Facility, Design Report, D.A.Edwards (editor), TESLA 95-01 (1995).

[5] K.T.Mc Donald, D.P.Russell, "Methods of Emittance Measurement", Proceedings of Joint US-CERN School in Observation, Diagnosis and Correction on Particle Beams, October 20-26 1988, Capri, Italy.

[6] E.Jenkins, SLC Memo 260 (1983).

[7] D.W.Rule, R.B.Fiorito, AIP Conference Proceedings 229 (1991) 315 ; Proceedings of 1993 Particle Accelerator Conference, May 1993, Washington DC, p.2453; 1993 Faraday Cup Award Invited Paper, Proceedings of Beam Instrumentation Workshop, Conf.Proc.No. 319 (1994) 21.

[8] M.L.Ter-Mikaelian, *High-Energy Electromagnetic Processes in Condensed Media* (Wiley-Interscience, 1972).

[9] S.G.Lipson, H.Lipson, *Optical Physics* (Cambridge Univ. Press 1969) §11.2.2.

[10] L.Wartski, Thése de doctorat d'Etat, Univ. Paris-Sud (1976).

[11] J.D.Jackson, *Classical Electrodynamics* (J.Wiley & Sons, 1975); W.Panofsky, M.Philipps, *Classical Electricity and Magnetism* (Addison-Wesley, 1962).

[12] V.Berestetskii, E.Lifshitz, L.Pitayevskii, *Quantum Electrodynamics* (Pargamon Press, 1982).

[13] K.Honkavaara et al., "Investigations on Diffraction Limitations on OTR Resolution", to be published.

[14] V.A.Lebedev, Nucl.Inst.Meth. A372 (1996) 344.

[15] D.Giove, A.Variola, "Analysis of the Main Characteristic Functions for the Optical Beam Diagnostics", to be published.

[16] W.B.Wetherell, "The Calculation of Image Quality", *Applied Optics and Optical Eng., Vol.VIII* (1980).

[17] Melles Griot Catalogue 1995/1996.

[18] X.Artru et al., "Experimental Investigations on Geometrical Resolution of Electron Beam Profiles Given by OTR in the GeV Energy Range", Proceedings of 5th European Particle Accelerator Conference, June 1996, Sitges, p.1686.

Parameter	$\lambda = 450$ nm	$\lambda = 650$ nm
ρ	176 ± 12 μm	163 ± 25 μm
a	$(9 \pm 5) * 10^{-5}$	$(6 \pm 3) * 10^{-5}$
b	1.12 ± 0.09	1.12 ± 0.06

Table 1: Parameters given by a fit of Eq.(13) with the experimental data.

L1 focal = 1000 mm
L2 focal = 250 mm
Distance OTR radiator - L1 = 1000 mm
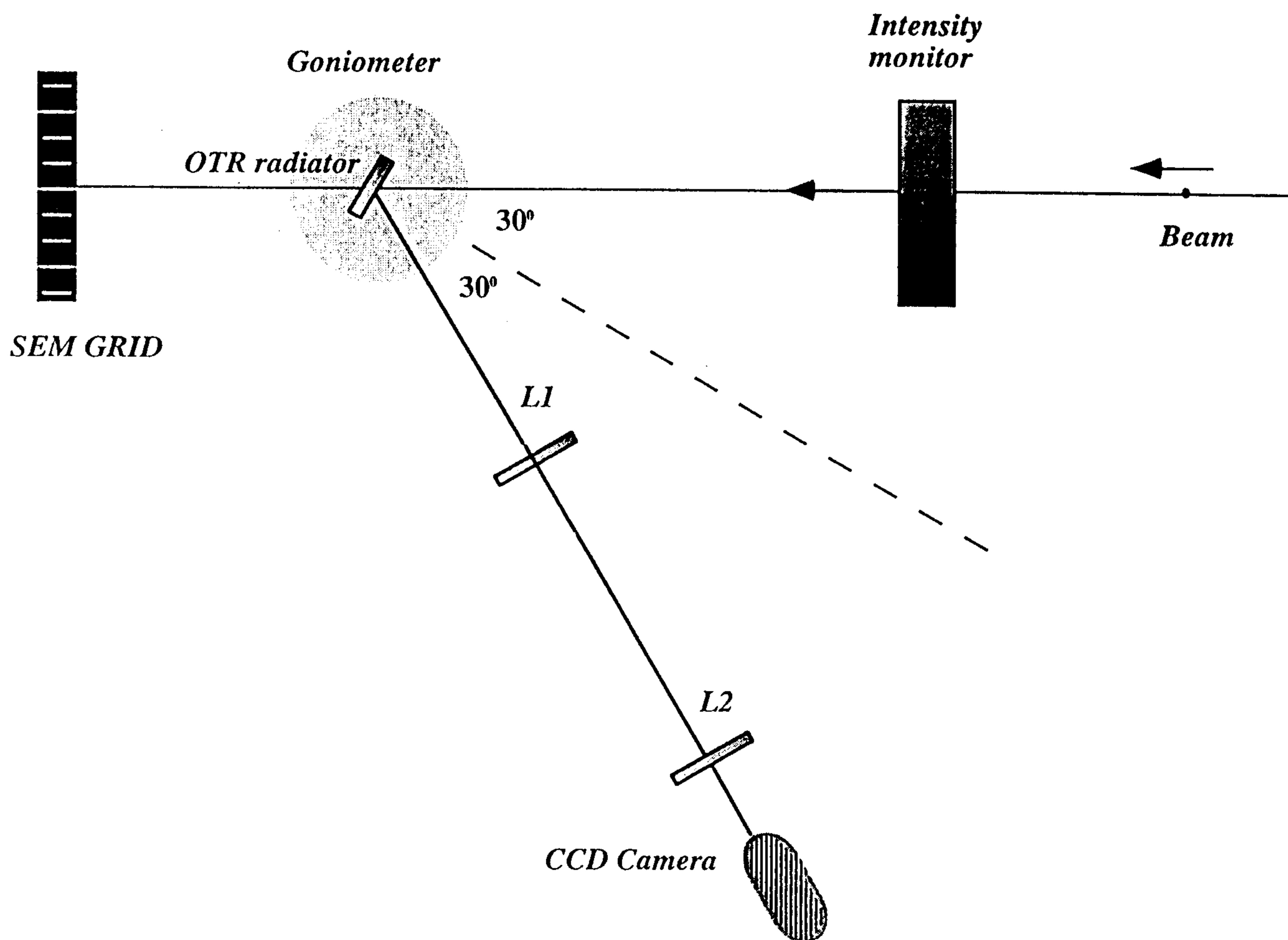*Distance L1 - L2 = 1250 mm*
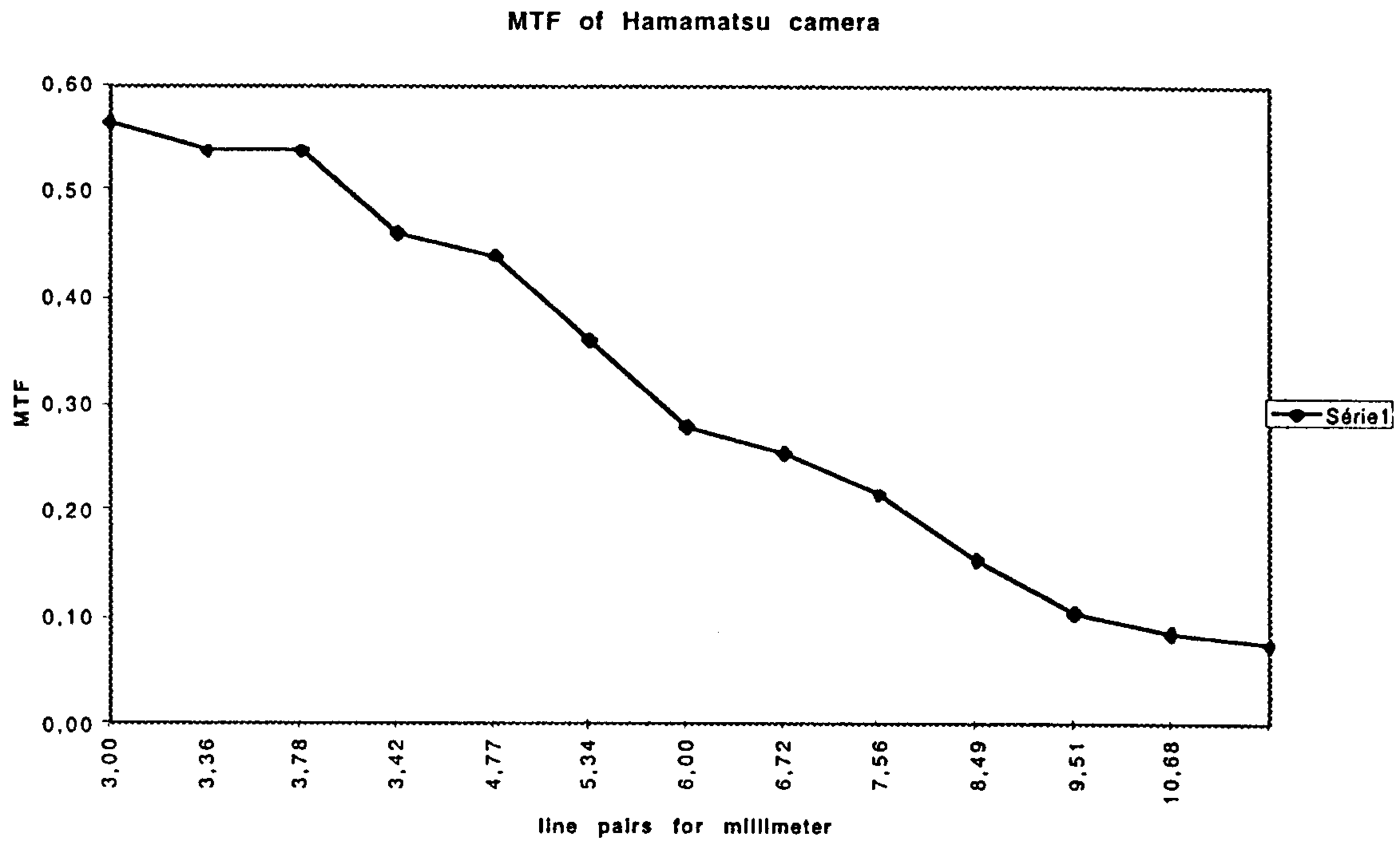*Distance L2 - CCD = 250 mm*

Figure 1: Experimental set-up.

MTF of Hamamatsu camera

Figure 2: Modulation Transfer Function of the used CCD camera.

Spot size vs. camera gain
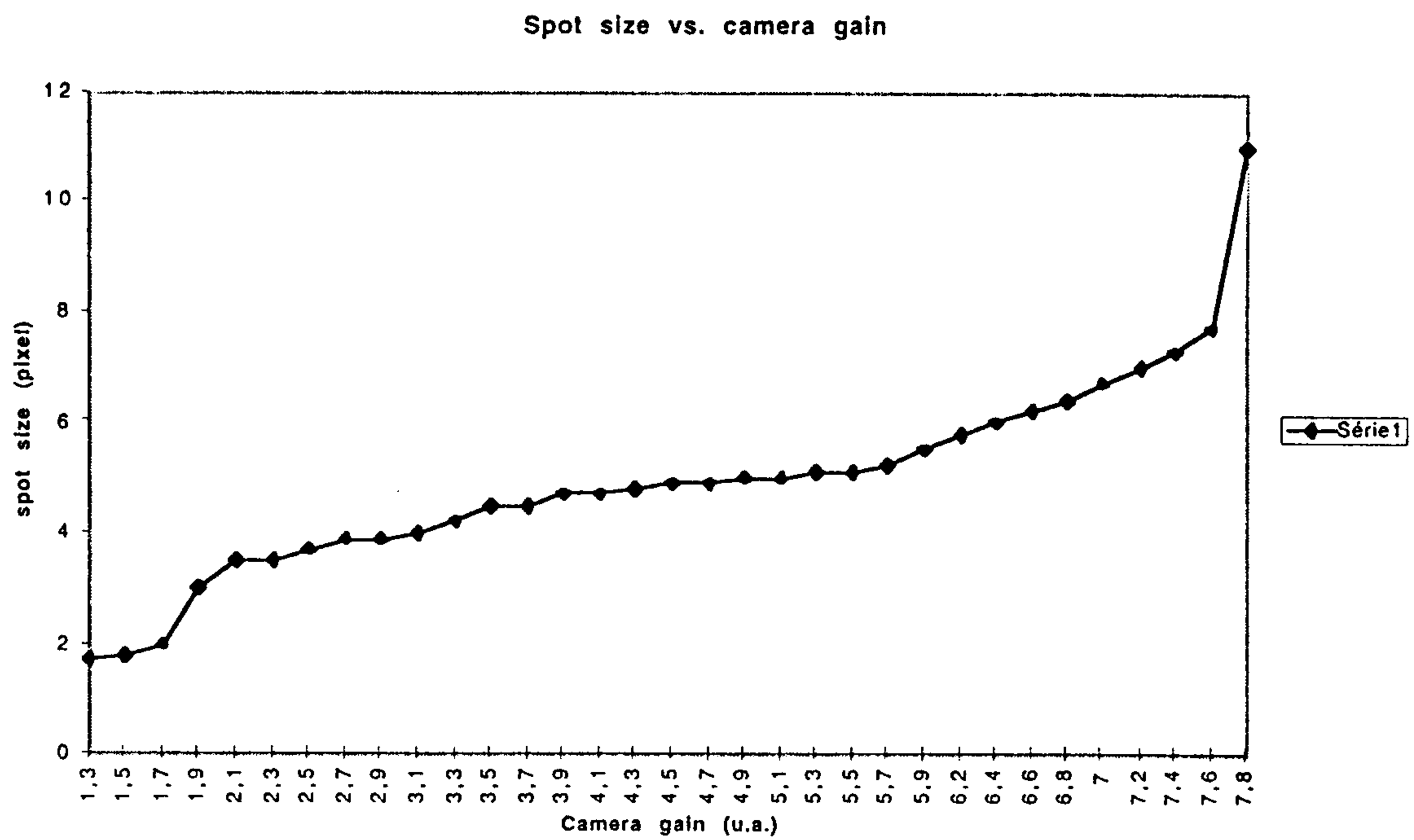
Figure 3: Spot size as a function of the camera gain.
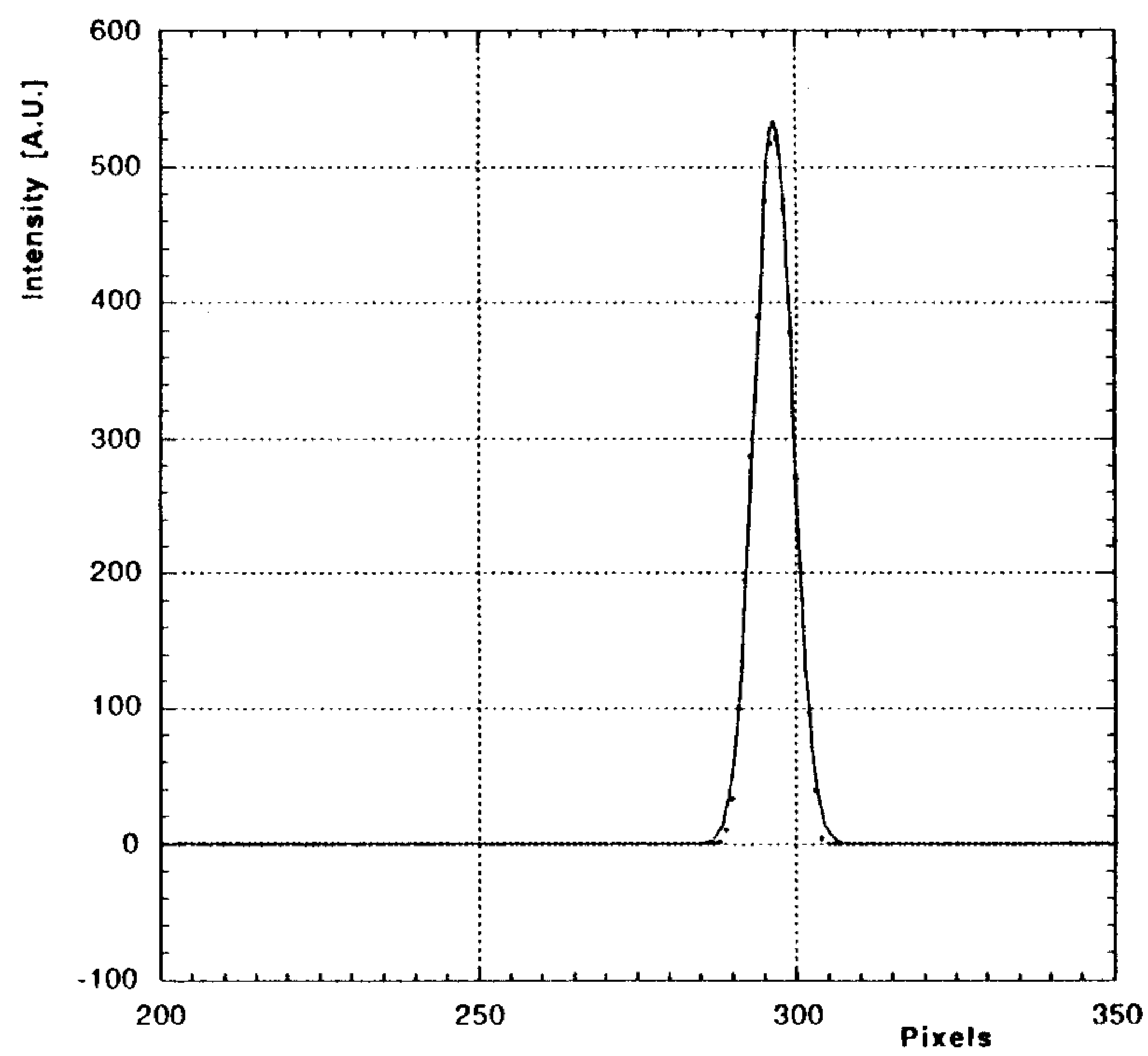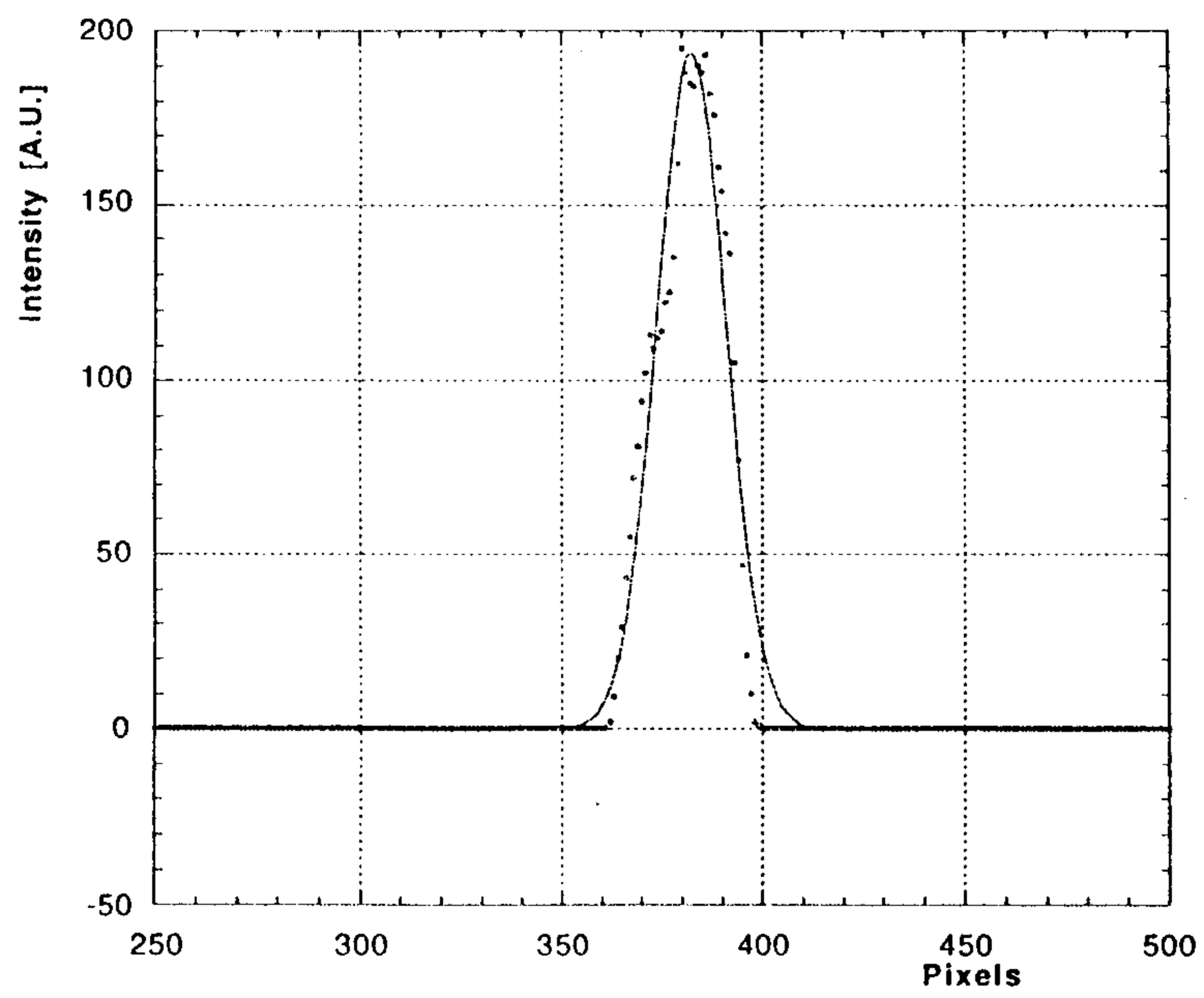
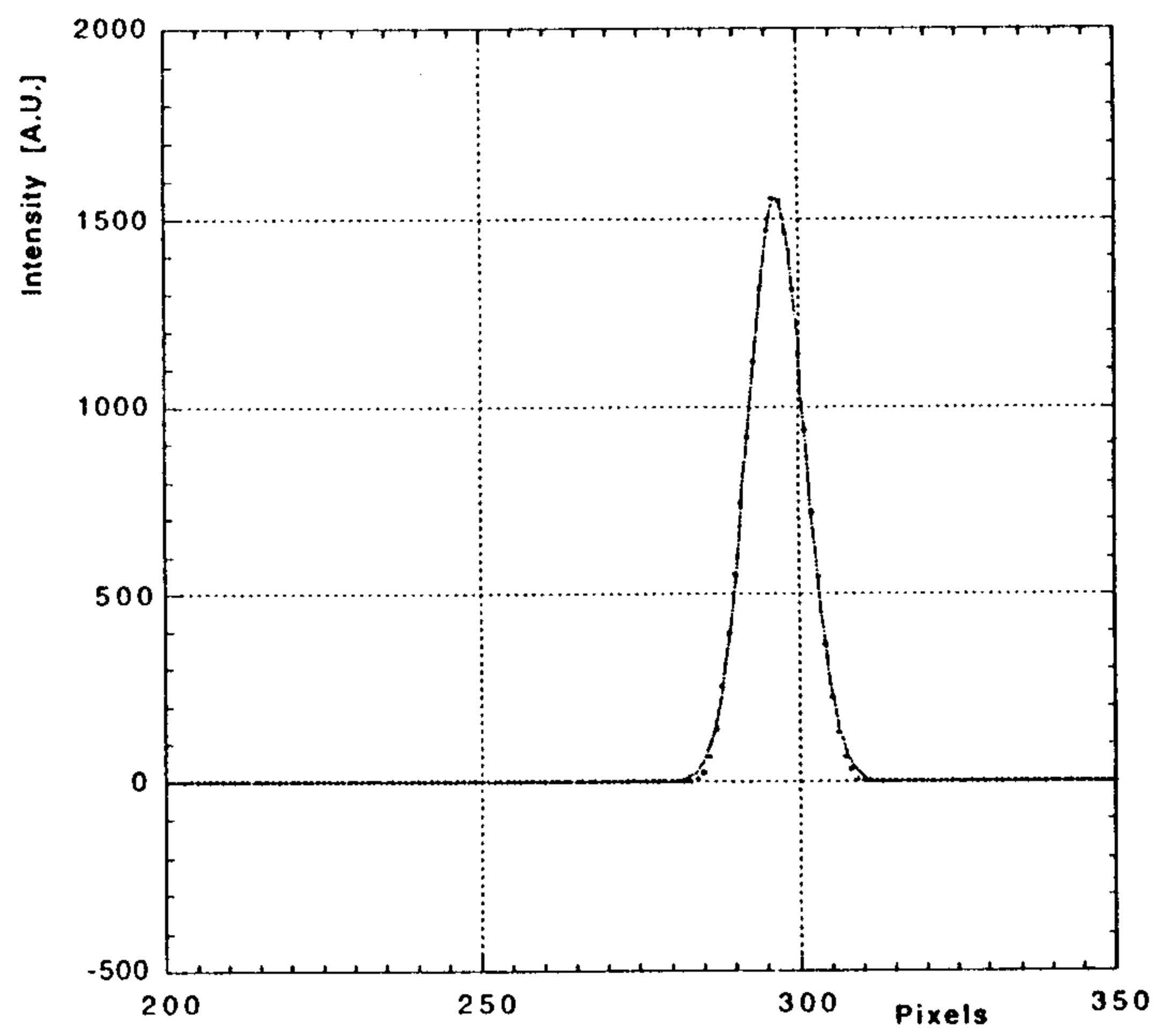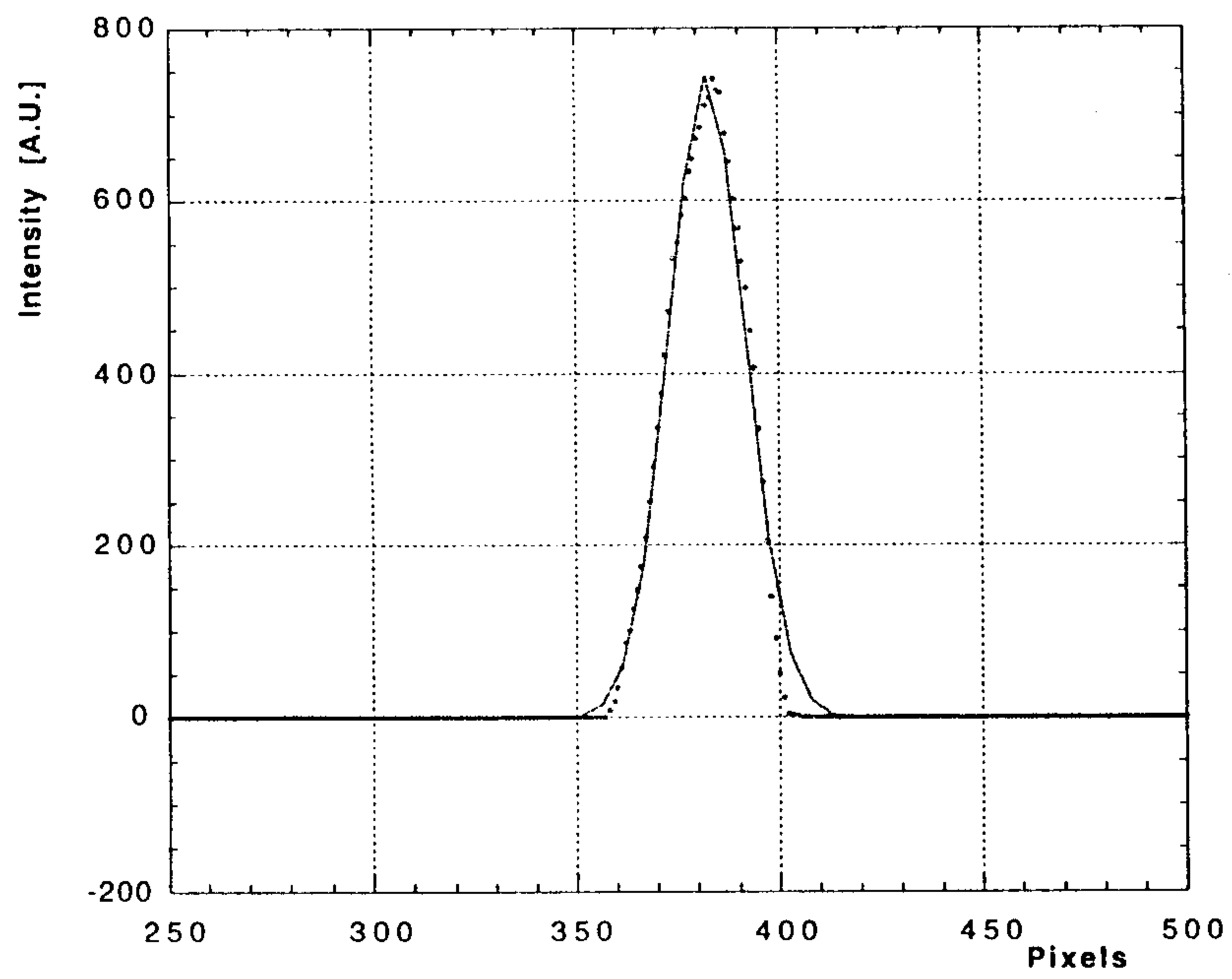Figure 4: Vertical and horizontal beam profiles at 2 GeV for a low camera gain.

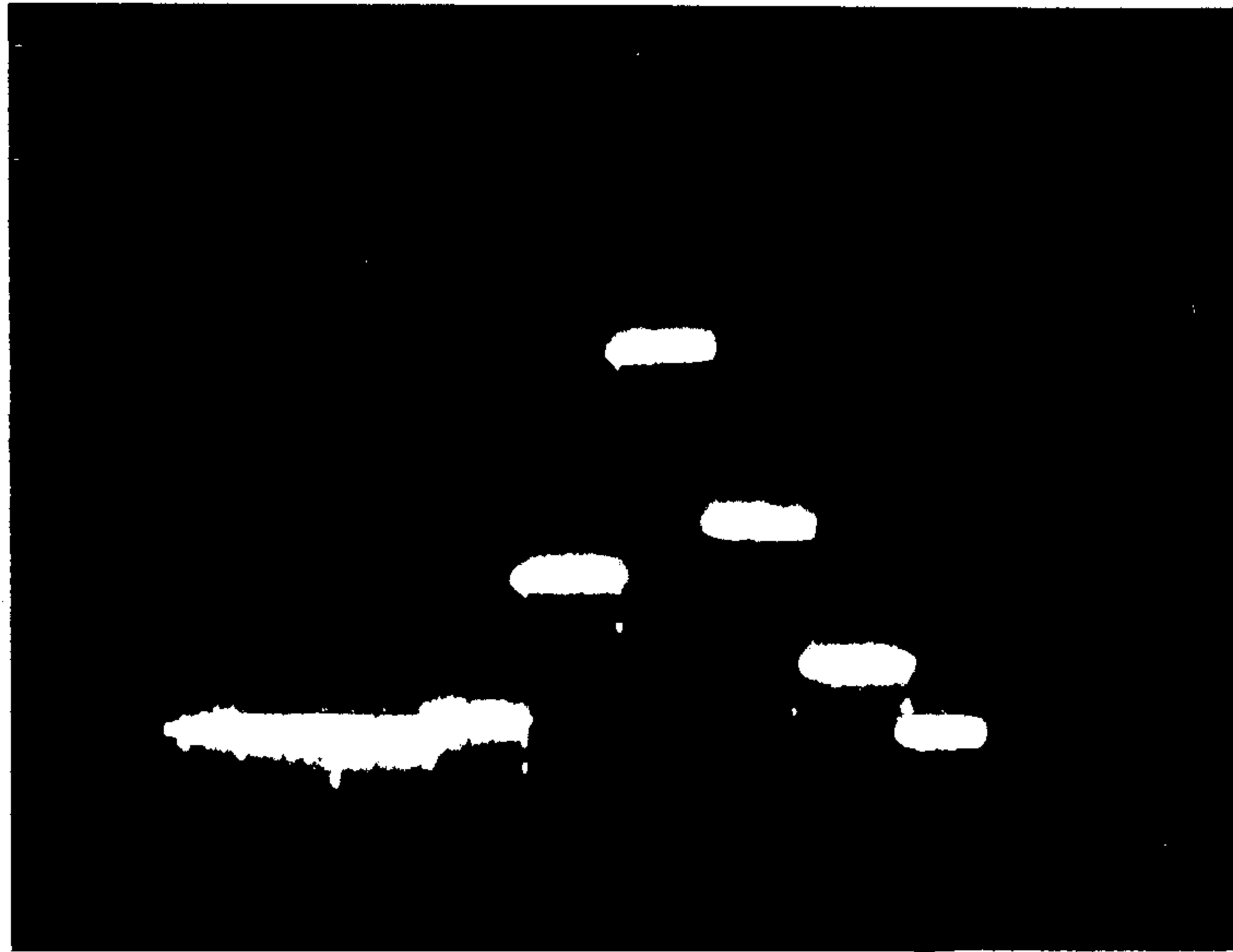Figure 5: Vertical and horizontal beam profiles at 2 GeV for a high camera gain.

Figure 6: Beam profile obtained by the SEM Grid at 2 GeV. Steps have a period of 0.5 mm.

Figure 7: Beam image at 2 GeV. The scale of the figure is 100x100 pixels (in horizontal direction 1 px = 0.097 mm and in the vertical direction 1 px = 0.064 mm; the different ratios are due to the frame grabber acquisition).
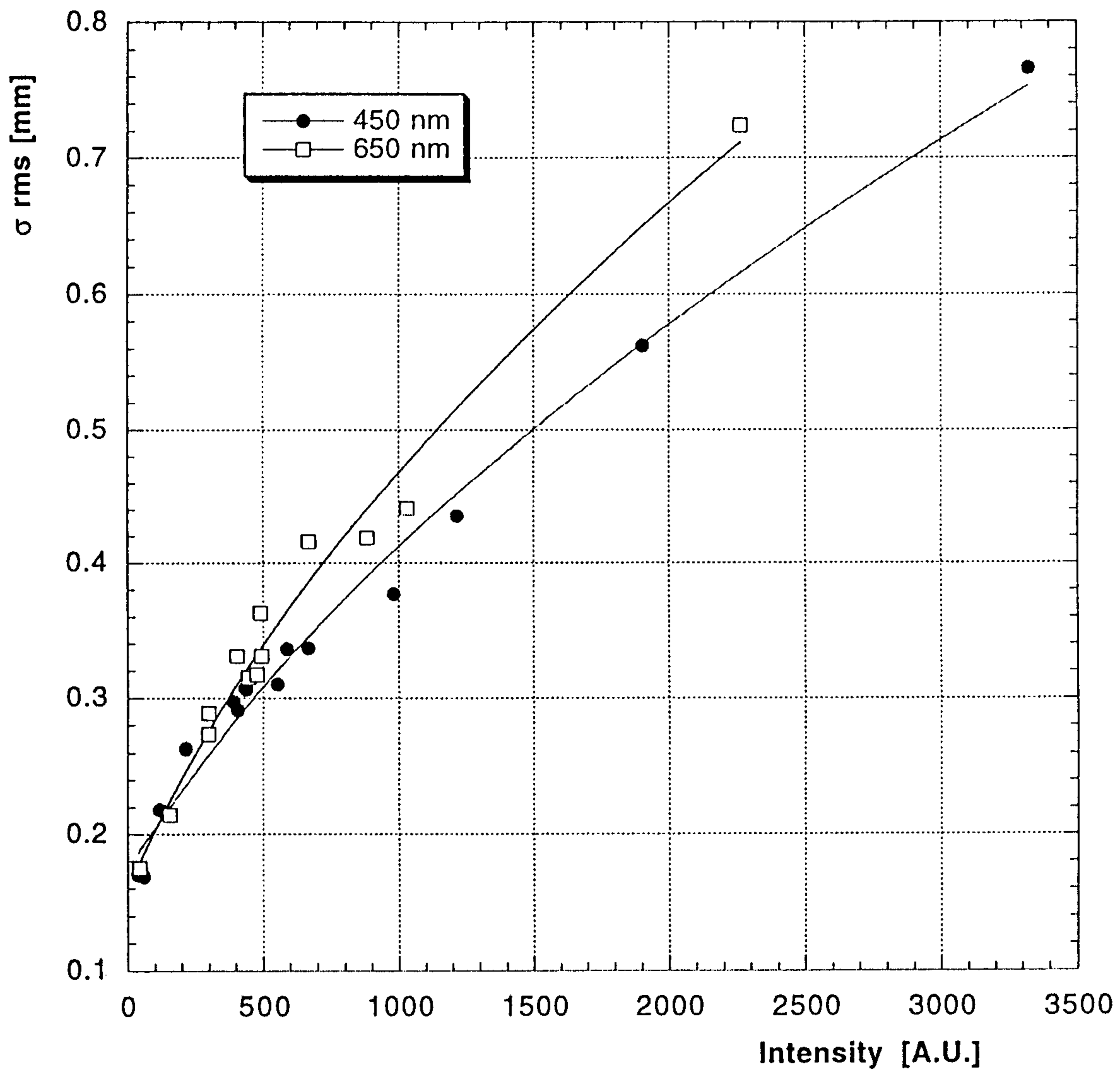
Figure 8: Measured rms beam size values as a function of the total intensity for $\lambda = 450$ nm and $\lambda = 650$ nm at 2 GeV. The continuous line is a fit of Eq.(13) with the experimental data.